Physica Medica 63 (2019) 35–40

Contents lists available at ScienceDirect

Physica Medica

journal homepage: www.elsevier.com/locate/ejmp

Technical note

The clinical significance of modifying X-ray tube current-time product based on prior image deviation index for digital radiography

Takeshi Takaki[a,b,*], Toshioh Fujibuchi[c], Seiichi Murakami[b], Takatoshi Aoki[d], Masafumi Ohki[c]

[a] Department of Health Sciences, Graduate School of Medical Sciences, Kyushu University, 3-1-1 Maidashi, Higashi-ku, Fukuoka 812-8582, Japan
[b] Department of Radiology, Hospital of University of Occupational and Environmental Health, Iseigaoka 1-1, Yahatanishi-ku, Kitakyushu-shi, Fukuoka 807-8555, Japan
[c] Department of Health Sciences, Faculty of Medical Sciences, Kyushu University, 3-1-1 Maidashi, Higashi-ku, Fukuoka 812-8582, Japan
[d] Department of Radiology, University of Occupational and Environmental Health School of Medicine, Iseigaoka 1-1, Yahatanishi-ku, Kitakyushu-shi, Fukuoka 807-8555, Japan

ARTICLE INFO

Keywords:
Deviation index
Statistical quality control
Portable X-ray digital radiography

ABSTRACT

Purpose: The absorbed dose at the image receptor in digital X-ray systems increases with an incorrect adjustment of the X-ray tube current-time product (mAs). Accordingly, the exposure index, target exposure index, and deviation index (DI) are proposed as absorbed dose optimization tools. We aimed at reducing the variation of DI in a short period by employing the mAs value determined by previously used mAs and DI.
Methods: We developed software that automatically calculates mAs for subsequent X-ray examinations based on mAs and DI values from prior examinations. Portable chest X-ray examinations in an intensive care unit (ICU) were performed for 16 weeks. The software was not used for the first 10 weeks in 406 cases and was used for the remaining 6 weeks in 216 cases. The changes in the non-conformance rate of DI for 16 weeks were evaluated using the p-chart used for quality control. The effect of the software on image noise was also evaluated.
Results: In total, 42% of cases had a DI range of −1 to 1 without using the software; this increased to 81% when using the software. Averages and variances of DI in cases with and without the software demonstrated statistically significant differences. From the p-chart, the non-conformance rate of DI was shown to decrease when using software. The software also worked for reducing the variation in image noise.
Conclusions: Our method reduced the variation in DI in a short period of time.

1. Introduction

Digital radiography (DR) imaging systems have gained popularity over screen and film systems. In general, flat-panel-detector (FPD) systems have been proven to reduce the absorbed dose delivered to the image receptor more than screen and film or computed radiography (CR) systems [1]. However, the absorbed dose delivered to the image receptor increases because of inappropriately chosen radiographic technique factors [2,3]. Many researchers have reported that a radiological technologist (RT) tends to increase exposure to avoid radiologist complaints about noisy images [4]; in particular, the X-ray tube current-time product (mAs) is not optimized in portable X-ray examinations in an intensive care unit (ICU) [3,5]. One of the causes of overexposure is that judging the optimal absorbed dose for the image receptor from X-ray images is difficult. Therefore, RTs have attempted to solve this problem by applying exposure indices suggested by the manufacturer [4]. However, manufacturers' exposure indices have led to confusion among RTs because they are based on several methods with different names (S value, REX value, EI value, etc.), calibration conditions, and mathematical forms [4]. The exposure index (EI), target exposure index (EIt), and deviation index (DI) were published as international standards intended to address this issue by the American Association of Physicists in Medicine and the International Electrotechnical Commission [4,6]. The measured and intended radiation exposures at the image receptor are given by EI and EIt, respectively. This means that both quantities are expressed in units of Air Kerma at the detector for a specific standard beam quality (RQA5) intended to simulate the quality of a beam exiting a normal adult abdomen. The EIt depends on the type of detector, type of examination, image quality (dependent on given clinical indications), and other parameters such as filtration and tube-voltage [4–9]. The DI is a measure of the difference between the EI and the EIt, and is defined as

* Corresponding author at: Department of Radiology, Hospital of University of Occupational and Environmental Health, Iseigaoka 1-1, Yahatanishi-ku, Kitakyushu-shi, Fukuoka 807-8555, Japan.
E-mail address: takaki-t@clnc.uoeh-u.ac.jp (T. Takaki).

https://doi.org/10.1016/j.ejmp.2019.05.011
Received 8 February 2019; Received in revised form 25 April 2019; Accepted 18 May 2019
Available online 28 May 2019

$$DI = 10 \cdot \log\left(\frac{EI}{EIt}\right) \quad (1)$$

The DI provides immediate feedback regarding the absorbed dose delivered to the detector. The DI also provides the operator with guidance on how the mAs should be adjusted for a repeated exposure of the same patient and view [10].

In recent years, with the spread of modality worklist management, DR systems automatically display a default mAs for a standard patient. However, for the absorbed dose delivered to image receptors to be constant, it is still necessary to adjust the radiographic technique factors according to individual patients' body thickness. This adjustment depends on the operator's technique. Al-Murshedi et al. reported that similar protocols were used for both standard and larger size patients; this was especially true when the examination was undertaken using manual exposure control compared with automatic exposure control (AEC) [11]; that is, as portable chest ICU imaging does not use AEC, the image quality can be inadequate [12,13]. Providing portable chest X-ray imaging with stable image quality by controlling radiographic technique factors has become an important issue. Gibson and Eslamy et al. attempted optimization of radiographic conditions using EI and DI with a CR system [3,14]. They conducted a manual process of adjusting the mAs from exposure indices recorded during prior examinations; therefore, considerable time was required to standardize the mAs (i.e., six weeks). Fitousi reported that the optimization and standardization of procedures and radiation doses are too complex to be accomplished using simple spreadsheets [15]. Furthermore, Gibson et al. concluded that by having a system in place to which RTs can refer during clinical practice, they can cross-check their own tendencies toward exposure setting [3]. However, current manufacturers do not provide software tools for portable X-ray systems to indicate recommended mAs based on prior image deviation index values. The purpose of this study is to reduce the variation of DI in a short period by employing the mAs value determined by previous mAs and DI values. The portable chest radiography was performed in the ICU of the Hospital of University of Occupational and Environmental Health (UOEH).

2. Materials and methods

2.1. Software for adjusting mAs

We developed software that extracted mAs and DI values from the Digital Imaging and Communications in Medicine (DICOM) header of the latest radiograph of individual patients; it also indicated the recommended mAs for subsequent X-ray imaging. MATLAB R2016b (MathWorks Inc., Natick, MA, USA) was used for software development. The software was installed on a laptop PC. When a patient ID is inputted, the latest examination date, tube voltage, recommended mAs value, and body thickness estimated from the height and weight are automatically displayed. In addition, the most recent X-ray image is displayed on the right side of the display as a reference for setting the exposure field size.

The flowchart for calculating the recommended mAs is shown in Fig. 1. As the operator inputs the corresponding patient ID, the software automatically extracts the latest radiograph and determines the mAs and DI values from the DICOM header. The mAs to be set from the second examination onward is calculated using the relationship between DI and the fraction of intended exposure (as a percentage) [10]. The software calculates the recommended mAs using the equation given below.

$$mAs_r = mAs_p \times EXP^{-0.23DI_p} \quad (2)$$

where mAs_r is the recommended mAs, mAs_p is the mAs obtained from prior examination, and DI_p is the DI obtained from prior examination. For example, if we use 4 mAs and a DI of + 1.6 was obtained, the software calculates 2.8 mAs.

2.2. Portable chest radiography in the ICU

The portable X-ray unit Sirius Starmobile tiara K (Hitachi Medical Co., Tokyo, Japan), AeroDR1717HQ (Konica Minolta Inc., Tokyo, Japan), and FPD and CS-7 (Konica Minolta Inc., Tokyo, Japan) diagnostic imaging workstations were used in this study. The specifications of the AeroDR1717HQ is described in Table 1. The software version for CS-7 was V1.22R01_011.

The radiographic conditions were a tube voltage of 80 kV and source to image-receptor distance of 120 cm. The default parameters were used for acquiring portable chest X-rays. A software-based scatter correction algorithm (Intelligent Grid, Konica Minolta Inc.) was applied to the images with grid ratios of 6:1. The FPD gain and offset and the uniformity calibration were verified before and during the study. The EI value was verified under standard RQA5 beam conditions [4,6]. The target EI was determined by taking the mean EI from 500 consecutive ICU chest radiographs of UOEH; its value was 250 [16].

The portable chest X-ray examinations were performed in an ICU for 16 weeks (13 May to 19 September 2017). The software we developed was not used for the first 10 weeks (406 cases), but was used for the remaining 6 weeks (216 cases). Our institutional review board approved this study and informed consent was waived.

2.3. Patient characteristics

The gender, age, weight, and height of patients were extracted from the DICOM header (Table 2). We also estimated patient body thickness using the equation given below [17].

$$T_{pat} = WT^{0.6} \times HT^{-0.8} \times 107.02 \quad (3)$$

where T_{pat} is estimated patient thickness (cm), WT is patient weight (kg), and HT is patient height (cm). This estimated patient thickness was used to calculate the entrance surface dose (ESD).

2.4. End-points

The mAs, DI, ESD, and standard deviation (SD) of the image were used as end-points. The mAs and DI values were extracted from the DICOM header, and the ESD was estimated by the non-dosimeter dosimetry method. The non-dosimeter dosimetry method estimates the ESD for a patient based on the factors that influence it (i.e., kV, mAs, filter, focus-skin distance, device used), and the result often agrees with the actual measured value [18].

$$\mathrm{ESD[mGy]} = \mathrm{NDD} - \mathrm{M(f)} * \mathrm{mAs} * (1/\mathrm{FSD})^2 \quad (4)$$

In the above equation, NDD-M(f) is a coefficient obtained from the relationship between tube voltage and total filtration, mAs is the tube current-time product, and FSD is the focus-skin distance. NDD-M(f) was set to 0.0972, and FSD is calculated using the equation given below.

$$\mathrm{FSD} = 120 - T_{pat} \quad (5)$$

In routine antero-posterior chest X-rays for patients at the ICU, the detection of complications associated with indwelling devices such as endotracheal tubes and central venous catheters is very important [19]. To identify these indwelling devices, a sufficient dose for the mediastinum is needed. For the evaluation of image quality, we considered the noise within the subdiaphragmatic area without ribs and vessels other than the mediastinum. The image noise was evaluated by the SD of the pixel values for the presentation image. More specifically, we manually set five regions of interest (ROI), of 50 × 50 pixels each, on the infradiaphragmatic area at random. These ROIs include nonuniform backgrounds such as gross anatomy of the blood vessels and the chest wall. To obtain an accurate quantitative noise measure of the subdiaphragmatic texture, we must correct for the nonuniform background in the ROIs. The background correction was performed by subtracting the background image values, obtained from a two-dimensional surface-

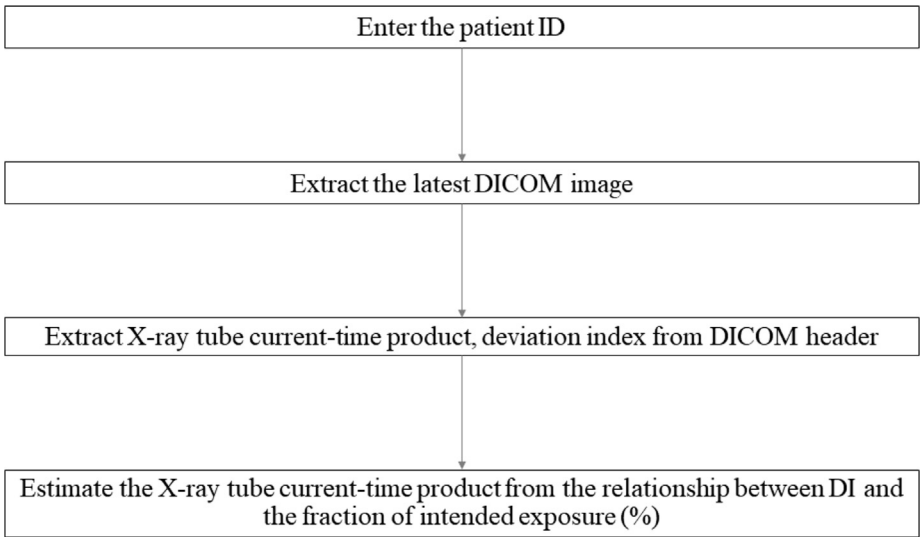

Fig. 1. Process flowchart for estimation of X-ray tube current-time product (mAs). As the operator inputs the corresponding patient ID, the software automatically extracts the latest radiograph and determines the mAs and deviation index (DI) values from the Digital Imaging and Communications in Medicine (DICOM) header. The mAs to be set from the second examination onward is calculated using the relationship between DI and the fraction of intended exposure (%).

Table 1
Technical specifications of the AeroDR1717HQ.

Wireless Digital Radiography System AeroDR	
Detection method	Indirect conversion method
Scintillator	CsI:TI (cesium iodide)
Dimensions	17″ × 17″ inches
Pixel size	175 μm
A/D conversion	16-bit
Dynamic range	10^4

Table 2
Patient information.

	Without adjusting mAs			With adjusting mAs		
	Range	Mean	S.D.	Range	Mean	S.D.
Age	18–92	63.6	14	18–93	63.9	17.8
Height (cm)	138–178	161.1	8.9	133–184	160.9	11.0
Weight (kg)	33.3–106.5	58.8	12.3	34–102.3	57.2	10.6

fitting technique, using the least squares method, from the original image [20]. Two-dimensional surface-fitting was performed using a two-dimensional second-order polynomial. The image noise was determined by calculating the SD using the trend-corrected image.

The statistical software, JMP 13 (SAS Institute Inc., Cary, NC, USA) was used for analysis. Welch's *t*-test was used because the F-test showed that the DI distributions were normal with unequal variances. A significance level of 5% was adopted in the F-test and Welch's *t*-test.

2.5. Proportion control chart

The changes in the conformance rate of DI for 16 weeks were evaluated using the p-chart used for quality control [21]. We defined 'non-conformant DI' as the proportion of DIs that were outside the target range of DI (between −1 and 1) with and without the software.

The non-conformant DI fractions (P_i) in each sample are calculated using the following equation:

$$P_i = \frac{x_i}{n_i} \tag{6}$$

where n_i is the size of each sample and x_i is the number of non-conformant DI in the sample i. The proportion control chart is generally managed by the following three lines: (1) central line, (2) variable upper control limit (UCL), and (3) variable lower control limit (LCL). The central line is calculated as follows:

$$\bar{P} = \frac{\sum_{i=1}^{k} x_i}{\sum_{i=1}^{k} n_i} \tag{7}$$

where k is the number of samples. The UCL and LCL lines are calculated as follows:

$$\mathrm{UCL} = \bar{P} + 3\sqrt{\frac{\bar{p}(1-\bar{p})}{n_i}} \tag{8}$$

$$\mathrm{LCL} = \bar{P} - 3\sqrt{\frac{\bar{p}(1-\bar{p})}{n_i}} \tag{9}$$

The ± 3 SD control limits capture a probability of 99.74% under normal distribution circumstances. The data for the average fraction of non-conformant DIs for each week were plotted as a control chart and the central line, UCL, and LCL were then calculated.

The non-conformant DI was evaluated using the proportion of the control chart plotted with the fraction of non-conformant DI each week.

3. Results

3.1. Patient characteristics

The mean body thicknesses for two groups with and without the software were 20.7 and 21.1 cm, respectively. There was no statistical difference between the two groups by gender and age ($p = 0.99$ and $p = 0.804$, respectively). The difference in the mean body thickness of the patients between the two samples were also not statistically significant ($p = 0.1034$).

3.2. End-Points

Table 3 presents results of the mAs, DI, ESD, and SD of images with and without adjusting the mAs. The differences in the average and the variance between the two distributions in mAs were statistically significant ($p < 0.0001$); the mAs showed large variation using the software compare with without the software. The DI decreased from 0.7 ± 1.7 to 0.2 ± 0.9, and the differences in the average and the variance between the two distributions in the DI was also statistically significant ($p < 0.0001$). The difference in the ESD was statistically significant ($p < 0.007$), and the average ESD was decreased by 10% using the software. The differences in the average between the two distributions of image noise were not statistically significant

Table 3
The mAs, DI, ESD, and SD of images with and without adjusting mAs in ICU portable chest X-ray examination.

	Without adjusting mAs (n = 406)	With adjusting mAs (n = 216)	Welch's *t*-test	F-test
mAs	2.1 ± 0.4	1.9 ± 0.8	$p < 0.0001$	$p < 0.001$
DI	0.7 ± 1.7	0.2 ± 0.9	$p < 0.0001$	$p < 0.001$
ESD (mGy)	0.22 ± 0.06	0.20 ± 0.10	$p < 0.007$	$p < 0.001$
SD of image	22.4 ± 6.6	22.2 ± 3.7	$p = 0.737$	$p < 0.001$

($p = 0.737$).

Fig. 2 presents the distribution of the deviation index with and without adjusting the mAs; the results show that the distribution of DI narrowed when using the software.

The percentages of cases in various DI ranges are shown in Table 4. The percentage of cases for which DI ranged from − 1 to 1 was 42% when not using the software (i.e., without adjusting mAs); this increased to 81% when using the software (i.e., adjusting the mAs).

3.3. Proportion control chart

In terms of the proportion control chart, the results of the average non-conformant DI for the conventional method and our developed software were 58% and 19%, respectively. The proportion control chart showed how using the software decreases the non-conformant DI. The differences in the two distributions of the fraction of non-conformant DI were statistically significant ($p < 0.001$; Fig. 3).

4. Discussion

Cohen et al. reported that 92% of exposures had a deviation index within the range of −3 to +3 and that these data established a practical reference range of exposure [22]. Seibert et al. reported that 73.5% of cases were within a target exposure range that corresponded to a DI range from −2 to 2 after education in radiographical technology [23]. We have also demonstrated similar results in that, without the use of software, 92% of exposures had a DI within the range of −3 to +3 and 70% of exposures had a DI within the range of −2 to 2. The SD of the DI was 1.7 (Cohen et al.'s result was 1.8). Generally, the distribution of DI narrows when using automatic exposure control [24]. Similarly, using the software to adjust mAs not only improved the mean of DI from 0.7 to 0.2, but also the SD of the DI reduced from 1.7 to 0.9. Therefore, we could improve efficiency at the ICU bedside using the proposed software.

Table 4
The percentage of cases in various DI ranges.

Deviation index range	−1 to 1	−2 to 2	−3 to 3	−4 to 4	−5 to 5
Without adjusting mAs	42	70	92	98	100
With adjusting mAs	81	97	100	100	100

There were a number of limitations in clinical practice when employing the mAs value determined by the previous mAs and DI values. The EI is calculated using a central value such as the median value of the histogram. Therefore, changes in the histogram owing to the presence or absence of a pleural effusion, differences in positioning and collimation, and the presence or absence of medical devices result in incorrect calculations of EI. These in turn lead to incorrect calculations of mAs. Second, the ROI was sometimes not set correctly for obtaining the histogram: the CS-7 sets the ROI automatically from the average vertical and horizontal profiles of chest X-ray images. However, the ROI might not have been recognized correctly in some cases for reasons such as incorrect positioning, inappropriate radiation field, artifacts, and so on. Consequently, the correct representative value could not be acquired and the correct EI was not calculated. Fig. 4 illustrates a case in which EI was not calculated correctly because of an inappropriate ROI.

5. Conclusions

A novel exposure adjustment software was developed. By using the software, it is possible to ascertain the required absorbed dose to be delivered to the detector in a second examination for each patient's body thickness from previous radiographic conditions and DI. As a result, it was possible to select the proper mAs value. In addition, the task of checking exposure indices and adjusting the radiographic technique factors based on the previous exposure condition became unnecessary

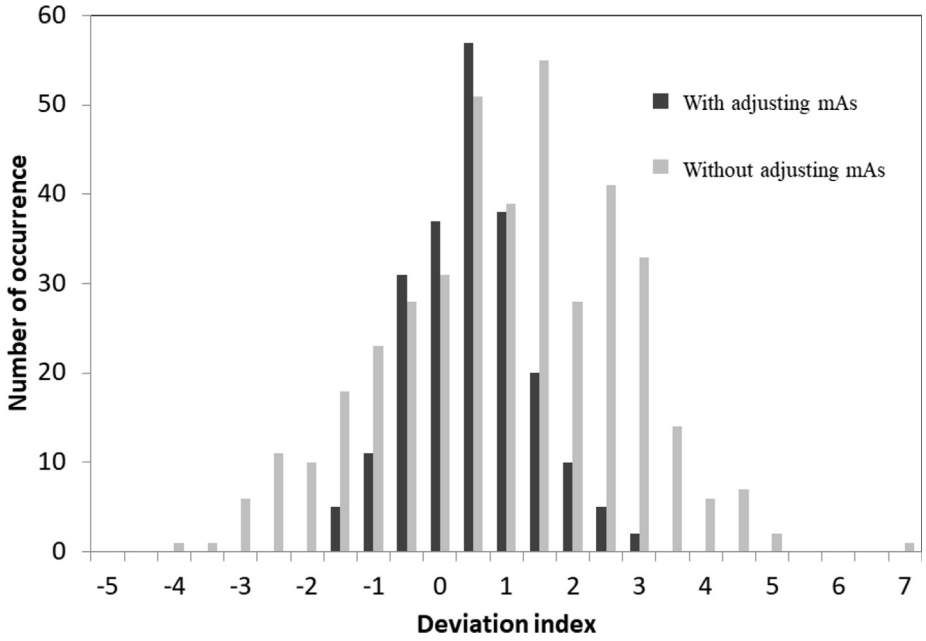

Fig. 2. Distribution of the deviation index with and without adjusting mAs in portable chest X-ray examination. The average of the deviation index (DI) with and without using the software was 0.2 ± 0.9 and 0.7 ± 1.7, respectively.

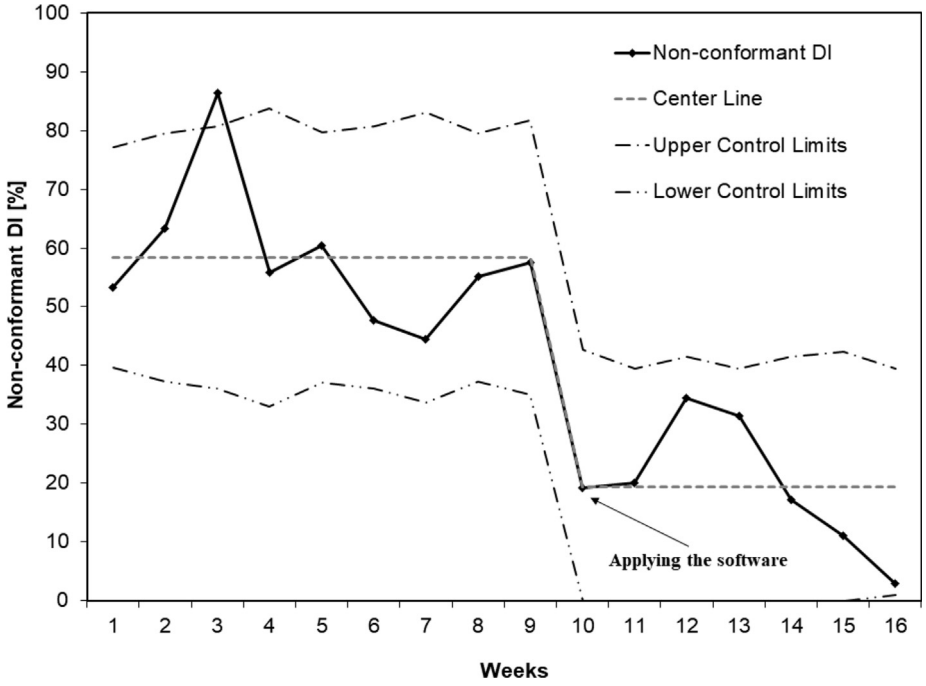

Fig. 3. Proportion control chart depicting the proportion of non-conformant deviation index (DI). The proportion control chart demonstrated how the new software decreased the non-conformant DI.

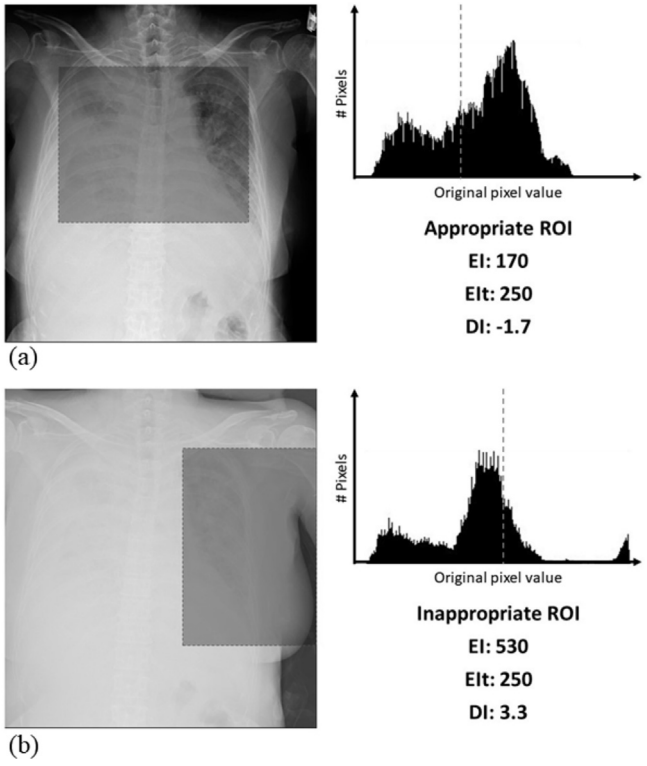

Fig. 4. Case in which the exposure index (EI) was not calculated correctly because of an inappropriate region-of-interest (ROI). Squares indicate different ROIs: (a) correctly recognized and (b) incorrectly recognized. Therefore, the value of interest for the wrong ROI (b) shifts to the right compared with the value of interest at the appropriate ROI and the EI is not calculated correctly.

when using the software. The radiographic technique factors could be set more effectively without relying on the experience of the RT. Variations in DI and image noise could be reduced in a short period of time. Further clinical study with this software is warranted to reduce patient exposure dose.

Acknowledgments

We would like to express our deepest gratitude to Dr. Yukunori Korogi, who provided us with this opportunity. We acknowledge the clinical staff of the Department of Radiology at the Hospital of the University of Occupational and Environmental Health for assistance with the data.

Declarations of interest

None.

Funding

This research did not receive any specific grant from funding agencies in the public, commercial, or not-for-profit sectors.

References

[1] Rong XJ, Shaw CC, Liu X, et al. Comparison of an amorphous silicon/cesium iodide flat-panel digital chest radiography system with screen/film and computed radiography systems - A contrast-detail phantom study. Med Phys. 2001;28:2328–35. https://doi.org/10.1118/1.1408620.
[2] Kishimoto K, Ariga E, Ishigaki R, et al. Study of Appropriate Dosing in Consideration of Image Quality and Patient Dose on the Digital Radiography. Japanese J Radiol Technol. 2011;67:1381–97.
[3] Gibson DJ, Davidson RA. Exposure creep in Computed Radiography: A Longitudinal Study. Acad Radiol. 2012;19:458–62. https://doi.org/10.1016/j.acra.2011.12.003.
[4] Shepard S, Wang J, Flynn M, et al. An exposure indicator for digital radiography. Report of AAPM Task Group 116. American Association of Physicists in Medicine. 2009. https://doi.org/10.1118/1.3121505.
[5] Don S. Radiosensitivity of children: potential for overexposure in CR and DR and magnitude of doses in ordinary radiographic examinations. Pediatr Radiol. 2004;34:167–72. https://doi.org/10.1007/s00247-004-1266-9.
[6] International Electrotechnical Commission. International Standard IEC 62494-1. Medical electrical equipment—exposure index of digital X-ray imaging systems—Part 1: definitions and requirements for general radiography. International Electrotechnical Commission. Geneva: International Electrotechnical Commission. 2008.
[7] Uffmann Matin, Schaefer-Prokop Cornelia. Digital radiography: The balance between image quality and required radiation dose. European J Radiol.

2009;72:202–8. https://doi.org/10.1016/j.ejrad.2009.05.060.
[8] Takaki T, Takeda K, Murakami S, et al. Evaluation of the effects of subject thickness on the exposure index in digital radiography. Radiol Phys Technol. 2016;9:116–20. https://doi.org/10.1007/s12194-015-0341-2.
[9] Yasumatsu S, Tanaka N, Iwase K, et al. Effect of X-ray beam quality on determination of exposure index. Radiol Phys Technol. 2016;9:109–15. https://doi.org/10.1007/s12194-015-0340-3.
[10] Willis CE, Don S. Advances in Chest Radiography Techniques: CR, DR, Tomosynthesis, and Radiation Dose Optimization. Pediatric Chest. Imaging. 2013. 1-12. 10.1007/174_2013_938.
[11] Al-Murshedi S, Hogg P, England A. Relationship between body habitus and image quality and radiation dose in chest X-ray examinations: a phantom study. Phys Med. 2019;57:65–71. https://doi.org/10.1016/j.ejmp.2018.12.009.
[12] Yamada K, Fujiwara T, Igari H, et al. Clinical Application of FCR (Fuji Computed Radiography) for the portable Chest Radiographs in ICU. Nihon Igaku Hoshasen Gakkai Zasshi. 1989;49:993–8.
[13] Busch HP. Digital radiography for clinical applications. European Radiol. 1997;7:66–72.
[14] Eslamy HK, Newman B, Weinberger E. Quality Improvement in Neonatal Digital Radiography: Implementing the Basic Quality Improvement Tools. Seminars in ULTRASOUND CT and MRI. 2014;35:608–26. https://doi.org/10.1053/j.sult.2014.08.002.
[15] Fitousi N. Patient dose monitoring systems: a new way of managing patient dose and quality in the radiology department. Phys Med. 2017;44:212–21. https://doi.org/10.1016/j.ejmp.2017.06.013.
[16] Cohen MD, Cooper ML, Piersall, et al. Quality assurance: using the exposure index and the deviation index to monitor radiation exposure for portable chest radiographs in neonates. Pediatr Radiol. 2011;41:592–601. https://doi.org/10.1007/s00247-010-1951-9.
[17] Ogawa K. Method of determining Body Thickness from Weight and Height. Nihon Hoshasen Gijutsu Gakkai Zasshi. 2009;65:50–6.
[18] Mori T, Muto H, Sato H, et al. Medical Exposures Based on the Survey of the X-ray Technical Conditions and the Proposal of Guidance Level. Nippon Igaku Hoshasen Gakkai Zasshi. 2000;60:389–95.
[19] Audin Craig R, Aran Shima, Muse Victorine V, Abbott Gerald F, Ackman Jeanne B, Sharma Amita, Wu Carol C, Kalra Mannudeep K, McLoud Theresa C, Shepard Jo-Anne O, Fintelmann Florian J, Gilman Matthew D. Bedside Chest Radiographs in the Intensive care Setting: Wireless Direct Radiography Compared to Computed Radiography. Curr Probl Diagn Radiol 2018;47(6):397–403. https://doi.org/10.1067/j.cpradiol.2017.09.008.
[20] Katsuragawa S, Doi K, MacMahon H, et al. Quantitative computer-aided analysis of lung texture in chest radiographs. Radiographics. 1990;10:257–69. https://doi.org/10.1148/radiographics.10.2.2326513.
[21] Duclos A, Voirin N. The p-control chart: a tool for care improvement. Intern J Quality in Health Care. 2010;22:402–7. https://doi.org/10.1093/intqhc/mzq037.
[22] Cohen MD, Markowitz R, Hill J, et al. Quality assurance: a comparison study of radiographic exposure for neonatal chest radiographs at 4 academic hospital. Pediatr Radiol. 2012;42:668–73. https://doi.org/10.1007/s00247-011-2290-1.
[23] Seibert JA, Shelton DK, Moore EH. Computed radiography X-ray exposure trends. Acad Radiol. 1996;3:313–8.
[24] Dave JK, Jones AK, Fisher R, et al. Current state of practice regarding digital radiography exposure indicators and deviation indices: Report of AAPM Imaging Physics Committee Task Group 232. Med Phys. 2018;45:1146–60. https://doi.org/10.1002/mp.13212.